



# Study on Setpoint Tracking Performance of the PID SISO and MIMO Under Noise and Disturbance for Nonlinear Time-Delay Dynamic Systems

Ali Rospawan, Yukai Yang, Po-Hsu Chen, Ching-Chih Tsai\*

Department of Electrical Engineering, National Chung Hsing University, Taichung, Taiwan

\*Correspondence: cctsai@nchu.edu.tw

SUBMITTED: 13 July 2022; REVISED: 30 September 2022; ACCEPTED: 2 October 2022

**ABSTRACT:** This paper presents a case study of the setpoint tracking performance of the proportional integral derivative (PID) controller on the Single-Input Single-Output (SISO) and Multi-Input Multi-Output (MIMO) nonlinear digital plants under Gaussian white noise and constant load disturbance for the nonlinear time-delay dynamic system. With the objective of getting a better understanding of the nonlinear discrete-time PID controller, we proposed a case study using two SISO and two MIMO digital plants, and then do the numerical simulations along with the addition of Gaussian white noise and load disturbance to simulate the real environment. In this paper, we compare the results of the system working with and without noise and load disturbance. The study result of this paper shows that on the discrete-time digital nonlinear plant, the PID controller is working well to follow the nonlinear setpoint even under heavy noise and load disturbance. The study compared the performance indexes of the controllers in terms of the maximum error, the Root mean square error (RMSE), the Integral square error (ISE), the Integral absolute error (IAE), and the Integral of time-weighted absolute error (ITAE).

**KEYWORDS:** PID; MIMO; SISO; nonlinear plant; integral index performance

---

## 1. Introduction

PID control is proportional, integral, and derivative control, respectively, and PID parameter tuning refers to tuning or adjusting the three-term PID gain parameters, proportional, integral, and derivative gain, to achieve the system's desired control impact. PID control optimization has long been regarded as a significant parameter search problem in industry and academia. Many researchers have introduced and applied advanced methods for tuning the PID gain parameter. The authors in [1], [2] introduce a self-tuning PID controller, and Tsai et al. [3] present a PID parameter tuning using the Radial Basis Function Neural Network (RBFNN) method for stretch PET blow molding machines. The author in [4] presents a predictive PID controller using an Output Recurrent Fuzzy Wavelet Neural Network (ORFWNN) method, which is an improvement from the method proposed by the author in [5], which presents a Fuzzy Wavelet Neural Network (FWNN) method for tuning the PID gain parameter. The

author in [6] presents a Fuzzy Broad Learning System (FBLS) method that implies the FBLS identifier for online parameter tuning along with its identification, and the author in [7] improved its control structure and named it the Recurrent Fuzzy Broad Learning System (RFBLS) method. The authors in [8–10] present an Output Recurrent Fuzzy Broad Learning System (ORFBLS) method for tuning the PID gain parameter, and recently, the author in [11] presents an improvement structure for the adaptive predictive ORFBLS-PID control method. In its applications, the PID controller has been applied to many systems. The author in [12] applied the PID controller in the development of a hot air dryer for automotive tampo printing parts, and the author in [13] applied the PID control for automatic temperature control system on a smart poultry farm. The more advanced application of PID control using an advanced method has also been presented by so many researchers. The author in [14] applied a neural network PID for extrusion barrels in a plastic injection molding machine. The author in [9] applied the ORFBLS-APPID control for the chemical heating process in a wafer cleaning machine of semiconductor manufacturing apparatus, and the author in [6] applied the adaptive predictive FBLS-PID control to the tool-grinding servo control system.

This paper proposed a case study of the setpoint tracking performance of the PID controller on the SISO (single input, single output) and MIMO (multi-input, multi-output) digital discrete-time plant output under Gaussian white noise and constant load disturbance for the nonlinear time-delay dynamic system, taking into account the advanced study for tuning the PID gain parameter and its wide application. The rest of the paper is described as follows. Section 2 describes the mathematical model and control theory of the PID controller. Section 3 describes the numerical simulation results for SISO and MIMO plants and does a comparison study of their controlled plant output with and without Gaussian white noise and load disturbance. Then the conclusion and future work are presented in Section 4.

## 2. Mathematical Model and Control

PID controller is a feedback controller to delivers the control output at desired levels by continuously calculating an error value as the differentiation between setpoint or desired output and system output or measured process variable. In its application, PID control is applied to two areas of the output plant, single-input single-output (SISO), and multi-input multi-output (MIMO) plant. Figure 1 depicts the PID controller structure for both SISO and MIMO systems with Gaussian white noise  $\varepsilon(k)$  and constant load disturbance  $v(k)$ .

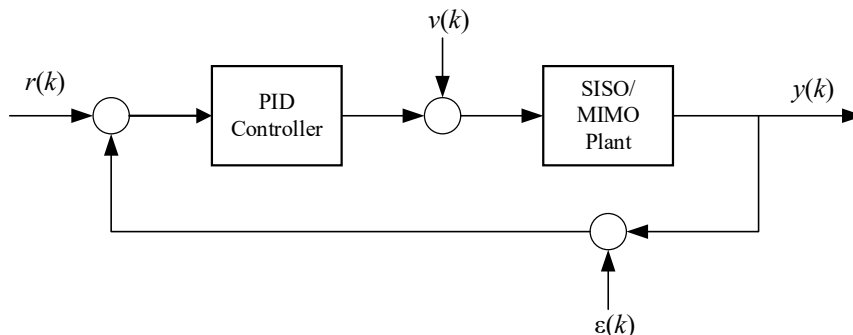


**Figure 1.** PID Controller structure with noise and disturbance

In industrial applications, PID controllers are mostly divided into 2 forms, the standard form, and the parallel form [15]. Equation (1) is the PID standard form and equation (2) is the PID parallel form. The PID standard form is the most relevant for the tuning algorithm. In standard

form, the parameters are shown clearly with the summation inside the equation, which generate a new error as a future and past error compensator. The proportional gain error is the current error. The derivative gain error is the predicted error at  $T_d$  seconds in the future, and the integral error is an error in  $T_i$  seconds from the sum of all past errors [16].

$$u(t) = K_p \left( e(t) + \frac{1}{T_i} \int_0^t e(\tau) d\tau + T_d \frac{d}{dt} e(t) \right) \quad (1)$$

$$u(t) = K_p e(t) + K_i \int_0^t e(\tau) d\tau + K_d \frac{d}{dt} e(t) \quad (2)$$

In the parallel form, the PID parameters are related to the parameters of the standard form through integral gain,  $K_i = K_p/T_i$  and derivative gain  $K_d = K_p T_d$  and despite being more complex mathematically, this parallel form is more commonly used in the industry [16].

In the MIMO system, following that the controlled system has multiple inputs  $x(k) \in \mathfrak{R}^{m \times 1}$  and multiple outputs  $y(k) \in \mathfrak{R}^{p \times 1}$  with the control objective being to follow the setpoint or process values  $r(k) \in \mathfrak{R}^{p \times 1}$ . The tracking error can be obtained by following equation (3) below.

$$e(k) = r(k) - y(k) \quad (3)$$

Where  $e(k)$  denotes the error tracking,  $r(k)$  denote the setpoint and  $y(k)$  denote the system output at the  $k$ -number of sampling time. And the controller output is defined by

$$u(k) = K(k)E(k) \quad (4)$$

Where,  $K(k) \in \mathfrak{R}^{m \times 3}$  is the set of PID gain parameters  $[k_p(k) \ k_i(k) \ k_d(k)]$ , and  $E(k) \in \mathfrak{R}^{3 \times p}$  is the set of errors  $[e(k) \ \dot{e}(k) \ \ddot{e}(k)]^T$ . Following Newton's notation for differentiating each side of the PID controller gives

$$u(k) = k_p e(k) + k_i \dot{e}(k) + k_d \ddot{e}(k) \quad (5)$$

Where  $e, \dot{e}$  and  $\ddot{e}$  are the error matrix vector for each PID parameter gain with the details described in equations (6) – (8) respectively.

$$e = e(k) \quad (6)$$

$$\dot{e} = \sum_{k=1}^n e(k)T \quad (7)$$

$$\ddot{e} = \frac{e(k) - e(k-1)}{T} \quad (8)$$

And  $k_p, k_i$  and  $k_d$  are proportional gain, integral gain, and derivative of the PID controller gain respectively, and due to computational simulation in the MIMO system, this PID parameters gain is written in a diagonal form as follows.

$$k_p = \begin{bmatrix} k_{p_1} & 0 \\ 0 & k_{p_2} \end{bmatrix}, k_i = \begin{bmatrix} k_{i_1} & 0 \\ 0 & k_{i_2} \end{bmatrix}, k_d = \begin{bmatrix} k_{d_1} & 0 \\ 0 & k_{d_2} \end{bmatrix}$$

As for the SISO system, there is no need to form the value for each parameter and calculation in matrix form.

### 3. Numerical Simulations and Discussion

In this section, the PID control performance will be indexed using two SISO benchmarks and two MIMO benchmarks of the nonlinear digital time-delay dynamic systems. The performance index parameter is used to evaluate the transient and steady-state control performance of the PID controller. Therefore, the five performance indexes are detailed as follows.

$$\text{Max Error} = \max|r(k) - y(k)| \quad (9)$$

Root mean square error (RMSE) is a performance evaluation to evaluate how far the controller output values from the designated setpoint in form of the quadratic mean of these differences. The detailed equation of ISE is shown in Eq. (10).

$$\text{RMSE} = \sqrt{\frac{\sum_{k=1}^S (r(k) - y(k))^2}{S}} \quad (10)$$

Integral square error (ISE) is a performance evaluation method defined by integrating the square of system error  $e(k)$  over a designated period of sampling number [17]. The detailed equation of ISE is shown in Eq. (11).

$$\text{ISE} = \sum_{k=1}^S (r(k) - y(k))^2 \quad (11)$$

Integral absolute error (IAE) is a performance evaluation method defined from the integral of system error  $e(k)$  absolute values over a designated period of sampling number [17]. The detailed equation of IAE is shown in Eq. (12).

$$\text{IAE} = \int_0^{1000T} |e(t)| dt \cong \sum_{k=1}^S |r(k) - y(k)| T \quad (12)$$

Integral of time-weighted absolute error (ITAE) is a performance evaluation method defined from the integral of system error  $e(k)$  absolute values multiplied by its current sampling number over a designated period of sampling number [17]. The detailed equation of ITAE is shown in Eq. (13).

$$\text{ITAE} = \sum_{k=1}^S |r(k) - y(k)| T \cdot k \quad (13)$$

where  $T$  denotes the sampling period and  $S$  is the total number of samples. The simulation study also includes an investigation of the effect of load disturbances  $v(k)$  and Gaussian white noise  $\varepsilon(k)$  [16] on the close loop control systems employing PID controller.

### 3.1. SISO simulations result for case study 1

Following the nonlinear digital discrete-time time-delay dynamic system on [6], [10], [11], the simulation system plant model is described as

$$y(k) = y^3(k-1) - 0.2|y(k-1)|u(k-d) + 0.08u^2(k-d) + \varepsilon(k) + v(k) \quad (14)$$

Where the time delay  $d$  is set by 7 and the PID gain parameters are set as  $k_p = 0.6$ ,  $k_i = 0.1$  and  $k_d = 0.1$ . The numerical simulation was performed following five sets of reference inputs  $r(k)$ , with the parameter given by

$$r(k) = \begin{cases} 0 & 0 < k \leq d; \\ 0.4 & 250 < k \leq 500; \\ 0.3 & 750 < k \leq 1000; \\ 0.1 & d < k \leq 250; \\ 0.5 & 500 < k \leq 750; \end{cases}$$

To investigate the noise and disturbances rejection ability of the PID controller, the mathematical model (14) of the SISO case study 1 was added with a Gaussian white noise  $\varepsilon(k)$  and constant load disturbance  $v(k)$  with the following parameter is shown below.

$$v(k) = \begin{cases} 0, & 0 < k \leq 600 \\ 0.1, & 600 < k \leq 1000 \end{cases}$$

After the numerical simulation, Figure 2 shows the setpoint tracking simulation result and the controller input of the PID controller respectively under setpoint changes (a) without noise and load disturbances and (b) with noise and load disturbances after the 1000<sup>th</sup> sampling instants.

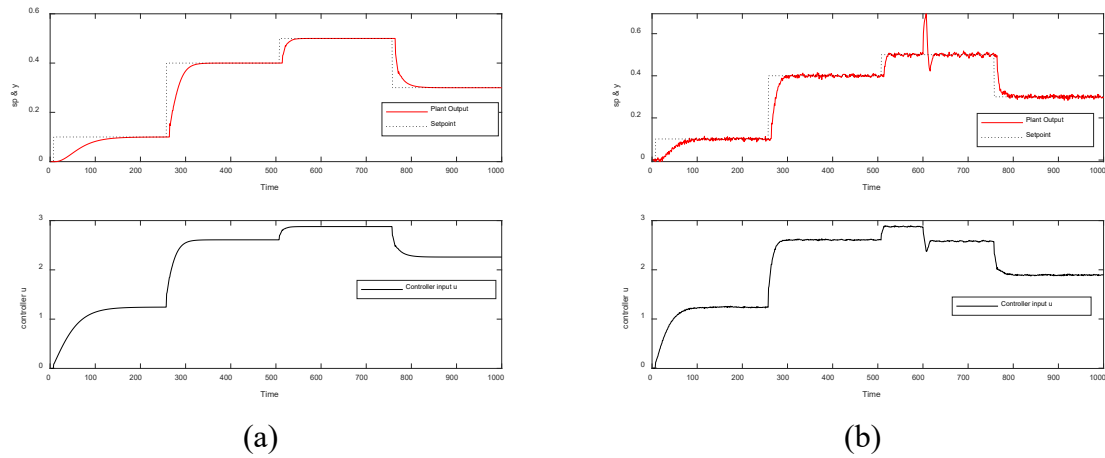


**Figure 2.** SISO case study 1 set point tracking and controller output result; (a) without noise and disturbance (b) with noise and disturbance

Figure 2(a) derived that without additional noise and disturbance, the plant output  $y(k)$  and controller output  $u$  signal shown smoothly compared with Figure 2(b) which showed noisily and has an overshoot signal starting at sampling number 600. These noisy signals are caused by additional gaussian white noise, and the overshoot signals are caused by additional load disturbance to simulate the real environment. Table 1 shows the performance of the PID controller in terms of maximum error, RMSE, ISE, IAE, and ITAE for both with and without noise and load disturbance.

**Table 1.** SISO Case study 1 controller performance

Controller	$v(k)$ & $\varepsilon(k)$	Max Error	RMSE	ISE	IAE	ITAE
SISO Case study 1	No	0.3000	0.0406	1.6508	11.7368	3439.8
SISO Case study 1	Yes	0.3073	0.0439	1.9301	17.2174	6717.1

In terms of the performance of the PID controller, adding the Gaussian white noise as natural noise and load disturbance highly impacted the controller which is shown in Table 1. Even though the difference between with or without noise and load disturbance is high especially in terms of ISE, IAE and ITAE, the controller is still able to maintain its stability to follow the designated setpoint. Note that the lower values of the index performance are the better results.

### 3.2. SISO simulations result for case study 2

Following the nonlinear digital discrete-time time-delay dynamic system on [6,10,11], the simulation system plant model is described as

$$\begin{aligned}
 y(k) = & 0.9722y(k-1) + 0.3578u(k-d) - 0.1295u(k-d-1) - 0.3103y(k-1)u(k \\
 & - d) \\
 & - 0.04228y^2(k-2) + 0.1663y(k-2)u(k-d-1) - 0.03259y^2(k-1)y(k-2) \\
 & - 0.3513y^2(k-1)u(k-d-1) + 0.3084y(k-1)y(k-2)u(k-d-1) \\
 & + 0.1087y(k-2)u(k-d)u(k-d-1) + \varepsilon(k) + v(k)
 \end{aligned} \tag{15}$$

Where the time delay  $d$  is set 3 and the PID gain parameters are set as  $k_p = 0.8$ ,  $k_i = 0.1$  and  $k_d = 0.2$ . The numerical simulation was performed following two sets of reference inputs  $r(k)$ , with the parameter given by

$$r(k) = \begin{cases} 1, & 0 < k \leq 500 \\ 0, & 500 < k \leq 1000 \end{cases}$$

To investigate the noise and disturbances rejection ability of the PID controller, the mathematical model (15) of the SISO case study 2 was added with a Gaussian white noise  $\varepsilon(k)$  and constant load disturbance  $v(k)$  with the following parameter is shown below.

$$v(k) = \begin{cases} 0, & 0 < k \leq 250 \\ 0.05, & 250 < k \leq 750 \\ 0.1, & 750 < k \leq 1000 \end{cases}$$

After the numerical simulation, Figure 3 shows the setpoint tracking simulation result and the control signal input of the PID controller respectively under setpoint changes (a) without noise and load disturbances (b) with noise and load disturbances after the 1000<sup>th</sup> sampling instants.

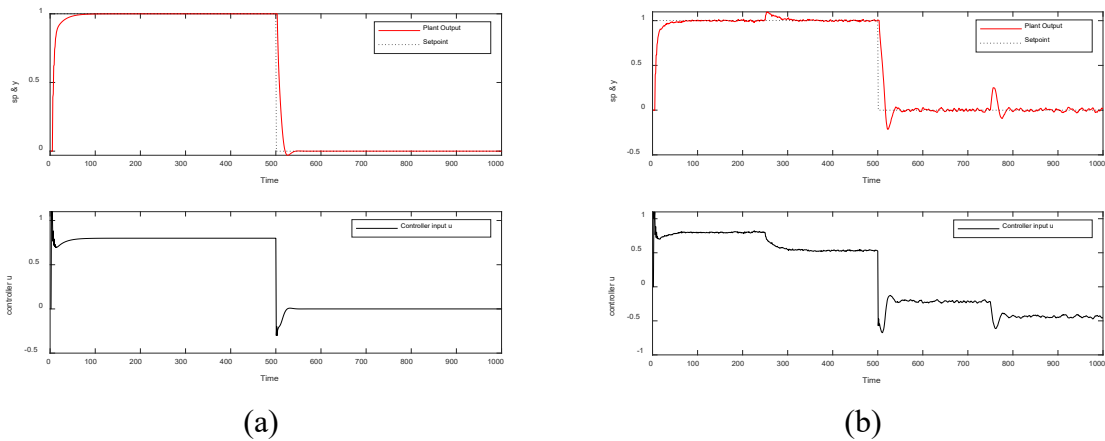


**Figure 3.** SISO case study 2 set point tracking and controller output result; **(a)** without noise and disturbance **(b)** with noise and disturbance

Similar to the result in Figure 2, the result shown in Figure 3(a) is shown smoothly compared with the result in Figure 3(b) which shown very noisy. These noisy signals are caused by additional gaussian white noise, and the overshoot signals are caused by additional load disturbance to simulate the real environment. The area with high overshoot is at sampling number  $k=250$  till  $k=270$  for the first stage of the setpoint, and the area at sampling number  $k=750$  till  $k=760$  for the second stage of the setpoint. Table 2 shows the performance of the controller regarding a max error, RMSE, ISE, IAE, and ITAE for both with and without noise and load disturbance.

**Table 2.** SISO Case study 2 controller performance

Controller	$v(k)$ & $\varepsilon(k)$	Max Error	RMSE	ISE	IAE	ITAE
SISO Case study 2	No	1.0004	0.1100	12.1001	18.7293	4535.1
SISO Case study 2	Yes	1.0041	0.1214	14.7491	35.2070	14227.4

In terms of the performance of the PID controller, adding the Gaussian white noise and load disturbance highly impacted the controller which is shown in Table 2. Even though the difference between with or without noise and load disturbance is high especially in terms of IAE and ITAE, the controller is still able to maintain its stability to follow the setpoint.

### 3.3. MIMO simulations result for case study 1

Following the nonlinear digital discrete-time time-delay dynamic system model on [18], the simulation system plant model for MIMO case study 1 is described as

$$\begin{aligned} y_1(k) &= \frac{a_1(k)y_1(k-1) + u_1(k-1)}{1 + y_1^2(k-1)} + \frac{0.5 * u_2(k-1)}{1 + u_2^2(k-1)} + \varepsilon(k) + v(k) \\ y_2(k) &= \frac{a_2(k)y_2(k-1) + u_2(k-1)}{1 + y_2^2(k-1)} + \frac{0.2 * u_1(k-1)}{1 + u_1^2(k-1)} + \varepsilon(k) + v(k) \end{aligned} \quad (16)$$

Where  $a_1(k) = 1.2(1 - 0.8e^{-0.5k})$  and  $a_2(k) = 1.2(1 - 0.8e^{-0.1k})$  are slowly time-varying plant models. Then, the PID gain parameters are set as given in the following parameter below.

$$\begin{array}{l} y_1(k) \\ \text{PID} \\ \text{Parameter} \end{array} \left\{ \begin{array}{l} \# \text{ of } d = 7 \\ \text{of } K_p = 0.8 \\ \text{of } K_I = 0.02 \\ \text{of } K_D = 0.1 \end{array} \right. , \begin{array}{l} y_2(k) \\ \text{PID} \\ \text{Parameter} \end{array} \left\{ \begin{array}{l} \# \text{ of } d = 7 \\ \text{of } K_p = 0.8 \\ \text{of } K_I = 0.08 \\ \text{of } K_D = 0.1 \end{array} \right.$$

The numerical simulation was performed following three sets of reference inputs  $r_1(k)$  and three sets of reference inputs  $r_2(k)$  with the parameter given by.

$$r_1(k) = \begin{cases} 0.1, & 0 < k \leq 250 \\ 0.4, & 250 < k \leq 500 \\ 0.5, & 500 < k \leq 1000 \end{cases}, r_2(k) = \begin{cases} 0.2, & 0 < k \leq 250 \\ 0.6, & 250 < k \leq 500 \\ 0.8, & 500 < k \leq 1000 \end{cases}$$

Figure 4 shows the setpoint tracking simulation result and the control signal input of the MIMO PID controller respectively under setpoint changes without noise and load disturbances. Figure 4(a) depicted the setpoint tracking and controller output for the plant output  $y_1$  and Figure 4(b) for the plant output  $y_2$ . The difference between these figures is the designated set point, wherein the first stage is 0.1 for  $y_1$ , 0.2 for  $y_2$ , and in its second stage on  $y_1$  is 0.4 and for  $y_2$  is 0.6 and on the last stage of setpoint, on  $y_1$  is 0.5 and for  $y_2$  is 0.8.

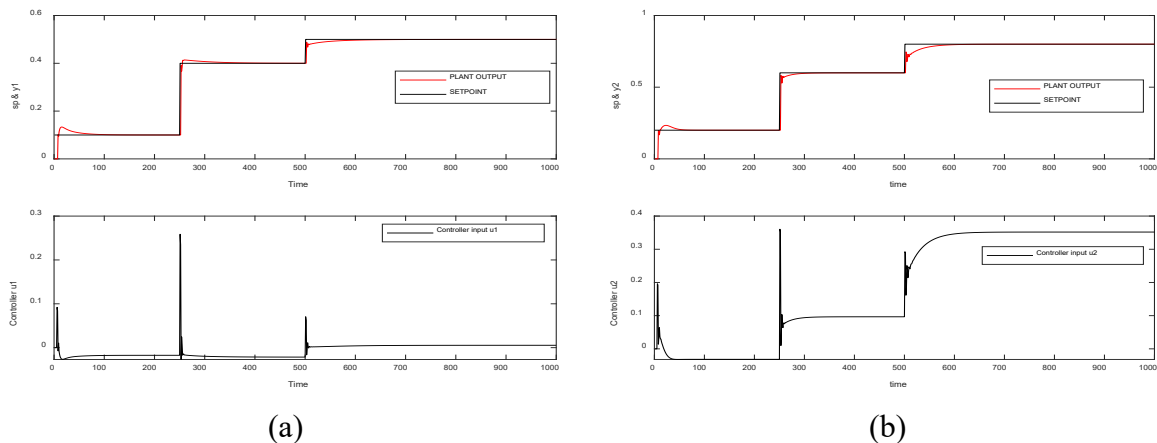


**Figure 4.** MIMO case study 1 set point tracking and controller output result without noise and disturbance; (a) Plant output 1 ( $y_1(k)$ ) (b) Plant output 2 ( $y_2(k)$ )

To investigate the noise and disturbances rejection ability of the PID controller, the mathematical model (16) of the MIMO case study 1 has been added with a Gaussian white noise  $\varepsilon(k)$  and constant load disturbance  $v(k)$  with the following parameter is shown below.

$$v(k) = \begin{cases} 0, & 0 < k \leq 250 \\ 0.05, & 250 < k \leq 750 \\ 0.1, & 750 < k \leq 1000 \end{cases}$$

Figure 5 shows the setpoint tracking simulation result and the control signal input of the PID controller respectively under setpoint changes with noise and load disturbances of variety amplitude after the 1000<sup>th</sup> sampling instant.

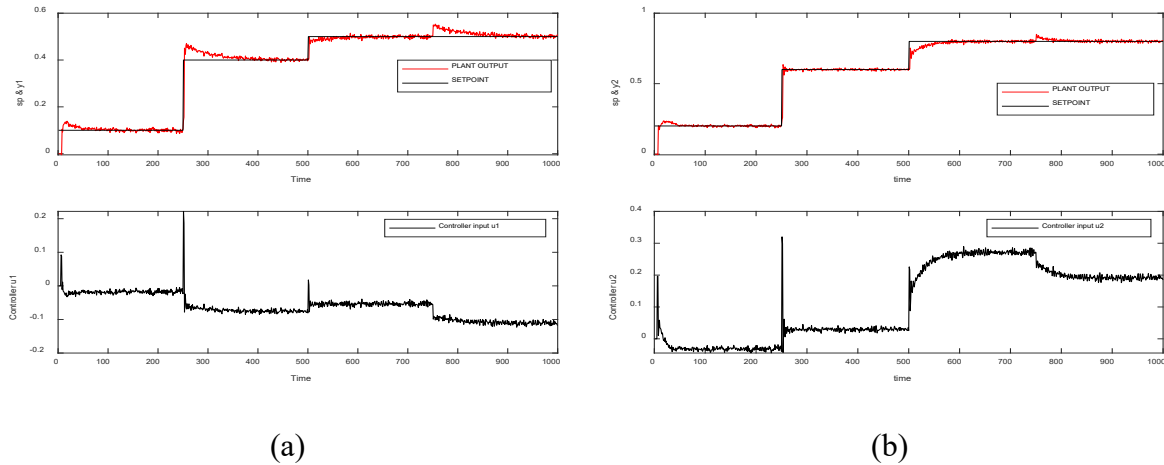


**Figure 5.** MIMO case study 1 set point tracking and controller output result with noise and disturbance; **(a)** Plant output 1 ( $y_1(k)$ ) **(b)** Plant output 2 ( $y_2(k)$ )

Figure 4 is shown smoothly compared with the result in Figure 5 which shown very noisy. These noisy signals are caused by additional gaussian white noise, and the overshoot signals are caused by additional load disturbance to simulate the real environment. During the first disturbance at  $k=250$  to  $k=750$  and the second disturbance at  $k=750$  to  $k=1000$ , the plant output  $y_2$  showed better than plant output  $y_1$ . This happens caused by its nonlinear plant itself (16), an initial PID gain parameters and the simulation model in equation (16). Table 3 indicates the performance of the controller regarding a max error, RMSE, ISE, IAE, and ITAE for both with and without load disturbance.

**Table 3.** MIMO Case study 1 controller performance

Controller	$v(k)$ & $\varepsilon(k)$	Max Error	RMSE	ISE	IAE	ITAE
MIMO Case study 1 Y1	No	0.3000	0.0176	0.3107	4.6397	1210.7
MIMO Case study 1 Y1	Yes	0.3440	0.0299	0.4489	11.3514	4963.3
MIMO Case study 1 Y2	No	0.4000	0.0292	0.8547	7.0804	2136.7
MIMO Case study 1 Y2	Yes	0.4520	0.0381	0.9707	10.5779	4406.0

In terms of the performance of the PID controller, adding the Gaussian white noise as natural noise and load disturbance highly impacted the controller which is shown in Table 3. Even though the error between with or without noise and load disturbance is high especially in terms of IAE and ITAE for plant  $y_1$  and only on ITAE for plant  $y_2$ , the controllers are still able to maintain their stability and keep following the designated setpoint. Note that the smaller value is better.



### 3.4. MIMO simulations result for case study 2

Following the nonlinear digital discrete-time time-delay dynamic system on [18,19], the simulation system plant model for MIMO case study 2 is described as

$$\begin{aligned}
 y_1(k+1) &= \frac{a_1 y_1(k-1) y_2(k-1)}{1 + a_2 y_1^2(k-1) + a_3 y_2^2(k-1)} + a_4 u_1(k-2) + a_5 u_1(k-1) + a_6 u_2(k-1) \\
 &\quad + \varepsilon(k) + v(k) \\
 y_2(k+1) &= \frac{b_1 y_2(k-1) \sin(y_2(k-2))}{1 + b_2 y_2^2(k-1) + b_3 y_1^2(k-1)} + b_4 u_2(k-2) + b_5 u_2(k-1) + b_6 u_1(k-1) + \varepsilon(k) + v(k)
 \end{aligned} \tag{17}$$

Where  $a_1 = 0.7, a_2 = 1, a_3 = 1, a_4 = 0.3, a_5 = 1$  and  $a_6 = 0.2$  for  $y_1$  plant output system parameter,  $b_1 = 0.5, b_2 = 1, b_3 = 1, b_4 = 0.5, b_5 = 1$  and  $b_6 = 0.2$  for  $y_2$  plant output system parameter. The PID gain parameters are set as given following parameter below.

$$\begin{array}{l}
 y_1(k) \\
 \text{PID} \\
 \text{Parameter}
 \end{array}
 \left\{ \begin{array}{l}
 \# \text{ of } d = 7 \\
 \text{of } K_P = 0.1 \\
 \text{of } K_I = 0.1 \\
 \text{of } K_D = 0.1
 \end{array} \right.
 \begin{array}{l}
 y_2(k) \\
 \text{PID} \\
 \text{Parameter}
 \end{array}
 \left\{ \begin{array}{l}
 \# \text{ of } d = 7 \\
 \text{of } K_P = 0.2 \\
 \text{of } K_I = 0.1 \\
 \text{of } K_D = 0.1
 \end{array} \right.$$

The numerical simulation was performed following four sets of reference inputs  $r_1(k)$  and four sets of reference inputs  $r_2(k)$  with the parameter given by

$$r_1(k) = \begin{cases} 0.1, & 0 < k \leq 250 \\ 0.4, & 250 < k \leq 500 \\ 0.5, & 500 < k \leq 1000 \end{cases}, \quad r_2(k) = \begin{cases} 0.2, & 0 < k \leq 250 \\ 0.6, & 250 < k \leq 500 \\ 0.8, & 500 < k \leq 1000 \end{cases}$$

Figure 6 shows the setpoint tracking simulation result and the control signal input of the MIMO PID controller respectively under setpoint changes without noise and load disturbances.

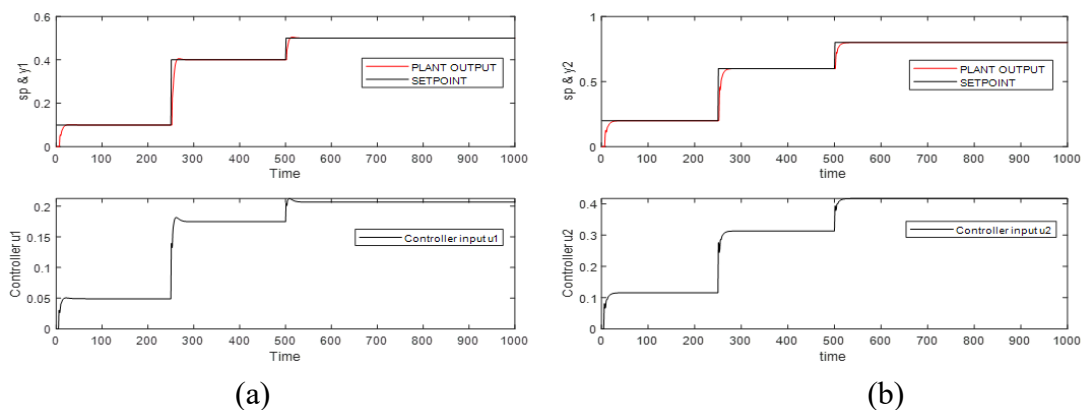


**Figure 6.** MIMO case study 2 set point tracking and controller output result without noise and disturbance; (a) Plant output 1 ( $y_1(k)$ ) (b) Plant output 2 ( $y_2(k)$ )

To investigate the noise and disturbances rejection ability of the PID controller, the mathematical model (17) of the MIMO case study 2 has been added with a Gaussian white noise  $\varepsilon(k)$  and constant load disturbance  $v(k)$  with the following parameter is shown below.

$$v(k) = \begin{cases} 0, & 0 < k \leq 250 \\ 0.05, & 250 < k \leq 750 \\ 0.1, & 750 < k \leq 1000 \end{cases}$$

Figure 7 shows the setpoint tracking simulation result and the control signal input of the PID controller respectively under setpoint changes with an addition of noise and load disturbances of variety amplitude after the 1000<sup>th</sup> sampling instant.

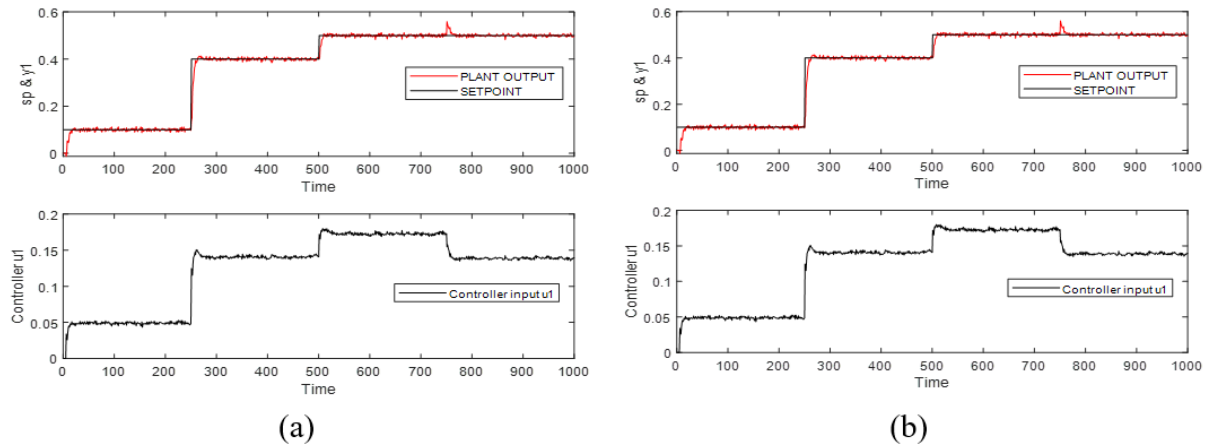


**Figure 7.** MIMO case study 2 set point tracking and controller output result with noise and disturbance; (a) Plant output 1 ( $y_1(k)$ ) (b) Plant output 2 ( $y_2(k)$ )

Figure 7 shown very noisy compared with Figure 6. These noisy signals are caused by additional gaussian white noise, and the overshoot signals are caused by additional load disturbance to simulate the real environment. The disturbance rejection of the PID controller on the MIMO case study 2 with the first disturbance at  $k=250$  to  $k=750$  and the second disturbance at  $k=750$  to  $k=1000$  showed similar results and both controller results are good. Table 4 indicates the performance of the controller regarding a max error, RMSE, ISE, IAE, and ITAE for both with and without load disturbance.

In terms of the performance of the PID controller, adding the Gaussian white noise as natural noise and load disturbance highly impacted the controller which is shown in Table 4. Even though the error between with or without noise and load disturbance is high especially in terms of IAE and ITAE for each plant output, the controllers are still able to maintain their stability and keep following the designated setpoint which is shown in Figure 7.

**Table 4.** MIMO Case study 2 controller performance

Controller	$v(k)$ & $\varepsilon(k)$	Max Error	RMSE	ISE	IAE	ITAE
MIMO Case study 2 Y1	No	0.3000	0.0194	0.3758	2.8522	1582.68
MIMO Case study 2 Y1	Yes	0.3585	0.0279	0.4219	6.6477	3827.8
MIMO Case study 2 Y2	No	0.4000	0.0301	0.9069	5.1640	1043.9
MIMO Case study 2 Y2	Yes	0.4588	0.0389	1.2343	14.7249	5362.2

#### 4. Conclusions

This paper presents a case study of the setpoint tracking performance of the PID controller on the SISO and MIMO nonlinear digital plants under Gaussian white noise and constant load disturbance for the nonlinear time-delay dynamic system. With the objective of getting a better understanding of the nonlinear discrete-time PID controller, we proposed a case study using two SISO and two MIMO digital plants, and then do the numerical simulations along with the addition of Gaussian white noise and load disturbance to simulate the real environment. In this

paper, we compare the results of the system working with and without noise and load disturbance. The study result of this paper shows that on the discrete-time digital nonlinear plant, the PID controller is working well to follow the designated nonlinear setpoint even under heavy noise and load disturbance. The result of PID controller performance on SISO Case Study 1 shows that, in terms of ISE, IAE, and ITAE have bigger errors compared with SISO Case Study 2, which is only on IAE and ITAE. MIMO Case Study 1 and MIMO Case Study 2 derived that only in terms of IAE and ITAE have big errors, which are almost twice their original controller performance value without Gaussian white noise and load disturbance. In future research, the PID controller can be used not only to nonlinear digital plants, but also to the real environment, and the noise and disturbance can be evaluated up to a particular threshold to determine the noise's aftereffect.

## Acknowledgments

The authors deeply acknowledge financial support from the Ministry of Science and Technology (MOST), Taiwan, ROC, under contract MOST 111-2622-8-005 -005 -TE1 and MOST 109-2221-E-005 -066 -MY2.

## References

- [1] Vega, P.; Prada, C.; Aleixandre, V. (2091). Self-tuning predictive PID controller. *IEEE Proceeding D (Control Theory and Application)*, 138, 303–312. <https://doi.org/10.1049/ip-d.1991.0041>.
- [2] Yamamoto, T.; Omatu, S.; Kaneda, M. (1994). A design method of self-tuning PID controllers. *Proceedings of 1994 American Control Conference*, 3, 3263–3267 <https://doi.org/10.1109/ACC.1994.735178>.
- [3] Tsai, C.C.; Chang, Y.L.; Tung, S.L. (2014). Two DOF temperature control using RBFNN for stretch PET blow molding machines. *2014 IEEE International Conference on Systems, Man, and Cybernetics (SMC)*, 1759–1764. <https://doi.org/10.1109/SMC.2014.6974171>.
- [4] Tsai, C.C.; Yu, C.C.; Tsai C.T. (2019). Adaptive ORFWNN-Based Predictive PID Control. *International Journal of Fuzzy System*, 21, 1544–1559. <https://doi.org/10.1007/s40815-019-00650-w>.
- [5] Tsai, C.C.; Tai, F.C.; Chang, Y.L.; Tsai, C.T. (2017). Adaptive Predictive PID Control Using Fuzzy Wavelet Neural Networks for Nonlinear Discrete-Time Time-Delay Systems. *International Journal of Fuzzy System*, 19, 1718–1730. <https://doi.org/10.1007/s40815-017-0405-z>.
- [6] Tsai, C.C.; Chan, C.C.; Li, Y.C.; Tai, F.C. (2020). Intelligent Adaptive PID Control Using Fuzzy Broad Learning System: An Application to Tool-Grinding Servo Control Systems. *International Journal of Fuzzy System*, 22, 2149–2162. <https://doi.org/10.1007/s40815-020-00913-x>.
- [7] Yang, C.H.; Tsai, C.C.; Tai, F.C. (2021). Adaptive Nonlinear PID Control Using RFBLs for Digital Nonlinear Dynamic systems. In *International Automatic Control Conference (CACS 2021)*, National Chung Cheng University, Chiayi, Taiwan, Nov. 2021.
- [8] Tsai, C.C.; Liou, G.L.; Tai, F.C. (2021). Adaptive Nonlinear Tracking Control Using Output Recurrent Fuzzy Broad Learning System for Digital Nonlinear MIMO Dynamic Systems. In *International Automatic Control Conference (CACS 2021)*, National Chung Cheng University, Chiayi, Taiwan, Nov. 2021.
- [9] Chou, C.Y.; Tsai, C.C.; Chen, H.S. (2020). Intelligent Adaptive PID Temperature Control Using Output Recurrent Fuzzy Broad Learning System: An Application to Chemical Heating Process in a Wafer Cleaning Machine. In *National Symposium on System Science and Engineering (NSSSE)*, National Chung Hsing University, Taichung, Taiwan, May 2020.

- [10] Hung G.S.; Tsai, C.C. (2021). Adaptive Nonlinear PID Control Using Output Recurrent Broad Learning System for Discrete-Time Nonlinear Dynamic Systems. *2021 International Conference on System Science and Engineering (ICSSE)*, 482–489. <https://doi.org/10.1109/ICSSE52999.2021.9538497>.
- [11] A. Rospawan, C. C. Tsai, and F. C. Tai, “Intelligent PID Temperature Control Using Output Recurrent Fuzzy Broad Learning System for Nonlinear Time-Delay Dynamic Systems,” presented at the 2022 International Conference on System Science and Engineering (ICSSE), National Chung Hsing University, Taichung, Taiwan, May 2022.
- [12] Rospawan, A.; Simatupang, J.W.; Purnama, I. (2022). Development of Hot Air Dryer Conveyor for Automotive Tampo Printing Parts. *Green Intelligent System and Application*, 2, 34–41. <https://doi.org/10.53623/gisa.v2i1.69>.
- [13] Enriko, I.K.A.; Putra, R.A.; Estananto (2021). Automatic Temperature Control System on Smart Poultry Farm Using PID Method. *Green Intelligent System and Application*, 1, 37-43. <https://doi.org/10.53623/gisa.v1i1.40>.
- [14] Tsai, C.C.; Lu, C.H. (2015). Adaptive Decoupling Predictive Temperature Control Using Neural Networks for Extrusion Barrels in Plastic Injection Molding Machines. *IEEE International Conference on Systems, Man, and Cybernetics*, 353–358. <https://doi.org/10.1109/SMC.2015.73>.
- [15] Åström, K.J. (2022). Control system design lecture notes for me 155a. University of California Santa Barbara, Santa Barbara, USA.
- [16] Ogata, K. (2009). *Modern Control Engineering*, Fifth Edition. New Jersey: Pearson Prentice Hall: New Jersey, USA.
- [17] Domański, P.D. (2020). *Control Performance Assessment: Theoretical Analyses and Industrial Practice*. Springer Nature: Switzerland. <http://doi.org/10.1007/978-3-030-23593-2>.
- [18] Zhang, M.G.; Wang, Z.G.; Wang, P. (2007). Adaptive PID decoupling control based on RBF neural network and its application. *2007 International Conference on Wavelet Analysis and Pattern Recognition*, 2, 727–731. <https://doi.org/10.1109/ICWAPR.2007.4420764>.
- [19] Taeib, A.; Ltaeif, A.; Chaari, A. (2013). A PSO Approach for Optimum Design of Multivariable PID Controller for nonlinear systems. *International Conference on Control, Engineering & Information Technology (CEIT'13) Proceedings Engineering & Technology*, 2, 206-210.



© 2022 by the authors. This article is an open access article distributed under the terms and conditions of the Creative Commons Attribution (CC BY) license (<http://creativecommons.org/licenses/by/4.0/>).